Contribution from the Departments of Chemistry, Northwestern University, Evanston, Illinois 60208, and Wabash College, Crawfordsville, Indiana 47933

Interaction of Metal Cluster Ketenylidenes, $[M_3(CO)_9(CCO)]^{2-}$ (M = Fe, Ru), with the Soft Electrophiles CuI and $CuPR_3^+$

Anuradha S. Gunale,[†] Michael P. Jensen,[†] David A. Phillips,[‡] Charlotte L. Stern,[‡] and Duward F. Shriver*,[†]

Received October 17, 1991

The reaction of $[Fe_3(CO)_9(C_\alpha C_\beta O)]^{2-}$ (I) with CuI yields a metal butterfly cluster III with the CCO ligand intact and Cu in a wingtip position. The X-ray structure determination also reveals a Cu–Cα distance of 2.008 (5) Å, and the ^{13}C NMR signal for C_α is deshielded by 113 ppm upon interaction with the Cu. The interaction of CuI with $[Ru_3(CO)_9(CCO)]^{2-}$ (II) is quite different. Again a 4-metal ketenylidene, IV, is produced, but the Cu atom now caps the triangle of the three Ru atoms on the face opposite from the CCO ligand. Both an X-ray structure determination and ^{13}C NMR spectra indicate no direct interaction between C_α and the copper. The greater basicity of ruthenium than iron may be responsible for the coordination of Cu^+ to all three metal atoms in the ruthenium ketenylidene and only two metal atoms of the iron ketenylidene. $[PPN]_2[Fe_3CuI(CO)_9(CCO)]$ (III) crystallizes in the triclinic space group $P\bar{1}$, (No. 2), with a = 11.863 (2) Å, b = 14.248 (4) Å, c = 23.807 (2) Å, α = 75.33 (2)°, β = 87.36 (2)°, V = 3888 (2) Å^3, and Z = 2. $[PPN]_2[Ru_3CuI(CO)_9(CCO)]$ (IV) crystallizes in the trigonal space group $P31c$ (No. 159), with $a = b$ = 13.655 (3) Å, c = 26.360 (6) Å, V = 4257 (2) Å^3, Z = 2.

Introduction

Triangular metal clusters containing the ketenylidene ligands (CCO) undergo a wide range of reactions including cluster building and transformations of the ketenylidene ligand.[1,2] For example, the reactions of anionic ketenylidenes $[M_3(CO)_9(CCO)]^{2-}$ (M = Fe, Ru, or Os) with electrophilic reagents often lead to cleavage of the C–CO bond.[2-6] Most of the electrophiles studied to date are either hard electrophiles such as H^+ and CH_3^+ or carbidophilic transition metals. In the present research, we explored the reactions of anionic ketenylidenes with the soft metal electrophile Cu^+.[7,8]

Experimental Section

General Procedures. All manipulations were carried out under a purified nitrogen atmosphere using standard Schlenk and syringe techniques or in a Vacuum Atmospheres drybox.[9] Solvents were collected and stored under nitrogen after refluxing and distilling from drying agents (CH_3CN from CaH_2, CH_2Cl_2 from P_2O_5, Et_2O from sodium benzophenone ketyl, and pentane from 4A sieves after predrying over concentrated H_2SO_4). The CD_2Cl_2 (99.5% D) used in NMR spectroscopy was freeze–pump–thaw degassed and vacuum-distilled from P_2O_5. The starting materials were synthesized by literature methods: $[PPN]_2[Fe_3(CO)_9CCO]$ (I)[6b,10] and $[PPN]_2[Ru_3(CO)_9(CCO)]$ (II)[4] were enriched to ca. 30% ^{13}C at all cluster carbons.

Solution IR spectra were recorded with Mattson Alpha Centauri, Nicolet 7199, and Bomem MB-series FTIR spectrometers over the frequency range from 2200 to 1500 cm^{-1} at 2-cm^{-1} resolution using a 0.1-mm path length CaF_2 window cell. ^{13}C NMR spectra were recorded on Varian XLA-400 spectrometer operating at 100.577 MHz. All chemical shifts are reported positive if downfield relative to TMS (0.00 ppm) with the ^{13}C resonance for CD_2Cl_2 (53.80 ppm) as an internal reference. Liquid secondary ion mass spectrometry experiments (colloquially FAB) were run by Dr. D. D. Hung of the Northwestern University Analytical Services Laboratory on a VG-70SE double-focusing high-resolution mass spectrometer. A *m*-nitrobenzyl alcohol matrix was used, and cesium iodide was the primary ion source. Negative ion detection was used to collect all the mass spectral data. Elemental analyses were performed by Elbach Analytical Laboratories (Engelskirchen, Germany).

Synthesis of $[PPN]_2[Fe_3CuI(CO)_9(CCO)]$ (III). A Schlenk flask was loaded with a 200-mg (0.13-mmol) sample of $[PPN]_2[Fe_3(CO)_9(CCO)]$ and 50 mg (0.13 mmol) of $[Cu(NCCH_3)_4][PF_6]$.[11] Acetonitrile (2.5 mL) was added, and the solution stirred for 10 min. A solution of 87 mg (0.13 mmol) of [PPN][I][12] in 1.5 mL of CH_3CN was added to the cluster mixture, which was stirred for another 10 min. The solution was evaporated to dryness, and the oily solids were extracted into CH_2Cl_2 (1.0 mL). Diethyl ether (7.0 mL) was slowly added until the desired dark brown product oiled out of solution. The $[PPN][PF_6]$ side product remained in solution and was removed by filtration. The cluster was redissolved in CH_2Cl_2 (3.0 mL), and the solution was layered with ether (15 mL) to afford dark brown crystals. These were isolated by filtration, washed with ether (8.0 mL), and dried in vacuo: 110 mg isolated; 49% yield. IR ν(CO) (CH_2Cl_2): 2024 (m), 1953 (s), 1877 (m) cm^{-1}. ^{13}C

Table I. Crystallographic Data

	$[PPN]_2[Fe_3CuI(CO)_9(CCO)]$ (III)	$[PPN]_2[Ru_3CuI(CO)_9(CCO)]$ (IV)
chem formula	$Fe_3CuICl_2P_4O_{10}C_{84}H_{62}N_2$	$Ru_3CuIP_4O_{10}C_{83}H_{60}N_2$
a/Å	11.863 (2)	13.655 (3)
b/Å	14.248 (4)	
c/Å	23.807 (2)	26.360 (6)
α/deg	75.33 (2)	
β/deg	87.36 (2)	
γ/deg	88.02 (2)	
V/Å^3	3888 (2)	4257 (2)
Z	2	2
fw	1812.22	1862.96
space group	triclinic $P\bar{1}$ (No. 2)	trigonal, $P31c$ (No. 159)
T/°C	−120	−120
λ(Mo Kα)/Å	0.710 73	0.710 73
ρ_{calc}/g cm^{-3}	1.548	1.453
μ/cm^{-1}	14.21	12.44
$R(F)^a$	0.038	0.073
$R_w(F)^b$	0.042	0.096

$^a R(F) = (\sum||F_o| - |F_c||)/\sum|F_o|$. $^b R_w(F) = [(\sum w|F_o| - |F_c|)^2/\sum wF_o^2]^{1/2}$. $w = 1/\sigma 2(F_o)$.

(1) Geoffroy, C. L.; Bassner, S. L. *Adv. Organomet. Chem.* **1988**, *28*, 1. (b) Seyferth, D. *Adv. Organomet. Chem.* **1976**, *14*, 97. (c) Sievert, A. C.; Strickland, D. S.; Shapley, J. R.; Steinmetz, G. R.; Geoffroy, G. L. *Organometallics* **1982**, *1*, 214. (d) Shapley, J. R.; Strickland, D. S.; St. George, G. M.; Churchill, M. P.; Bueno, C. *Organometallics* **1983**, *2*, 185. (e) Holmgren, J. S.; Shapley, J. R. *Organometallics* **1984**, *3*, 1322. (f) Mlekuz, M.; D'Agostino, M. J.; Kolis, J. W.; McGlinchey, M. J. *J. Organomet. Chem.* **1986**, *303*, 361.
(2) (a) Jensen, M. P.; Henderson, W.; Johnston, D. H.; Sabat, M.; Shriver, D. F. *J. Organomet. Chem.* **1990**, *394*, 121. (b) Hriljac, J. A.; Swepston, P. N.; Shriver, D. F. *Organometallics* **1985**, *4*, 158.
(3) Shriver, D. F.; Sailor, M. J. *Acc. Chem. Res.* **1988**, *21*, 374.
(4) Sailor, M. J.; Shriver, D. F. *Organometallics* **1985**, *4*, 1476.
(5) Went, M. J.; Sailor, M. J.; Bogdan, P. L.; Brock, C. P.; Shriver, D. F. *J. Am. Chem. Soc.* **1987**, *109*, 6023.
(6) (a) Jensen, M. P.; Sabat, M.; Shriver, D. F. *J. Cluster Sci.* **1990**, *1*, 75. (b) Hriljac, J. A.; Shriver, D. F. *J. Am. Chem. Soc.* **1987**, *109*, 6010.
(7) (A) Salter, I. D. *ADv. Organomet. Chem.* **1989**, *29*, 249. (b) Mingos, D. M. P. *Polyhedron* **1984**, *3*, 1289. (c) Evans, D. G.; Mingos, D. M. P. *J. Organomet. Chem.* **1982**, *232*, 171.
(8) A preliminary communication on a portion of this research has appeared: Gunale, A. S.; Jensen, M. P.; Stern, C. L.; Shriver, D. F. *J. Am. Chem. Soc.* **1991**, *113*, 1458.
(9) Shriver, D. F.; Drezdzon, M. A. *The Manipulation of Air-Sensitive Compounds*, 2nd ed.; Wiley: New York, 1986.
(10) Kolis, J. W.; Holt, E. M.; Shriver, D. F. *J. Am. Chem. Soc.* **1983**, *105*, 7307.
(11) Kubas, G. J. *Inorg. Synth.* **1979**, *19*, 90.
(12) Martinsen, A.; Songstad, J. *Acta Chem. Scand., A* **1977**, *31*, 645.

[†] Northwestern University.
[‡] Wabash College.

0020-1669/92/1331-2622$03.00/0

Table II. Positional Parameters for $[PPN]_2[Fe_3CuI(CO)_9(CCO)]$ (III)

	x/a	y/b	z/c
I	0.06702 (3)	0.87076 (3)	0.74029 (2)
Cu	0.03631 (6)	1.04239 (5)	0.73616 (3)
Fe1	−0.09635 (6)	1.18199 (6)	0.74721 (3)
Fe2	0.12050 (6)	1.19202 (6)	0.75680 (3)
Fe3	0.01100 (7)	1.32742 (6)	0.68599 (3)
O1	0.0718 (3)	1.2182 (3)	0.5851 (2)
O2	−0.2269 (3)	1.0057 (3)	0.7733 (2)
O3	−0.1099 (3)	1.2200 (3)	0.8626 (2)
O4	−0.2985 (4)	1.2930 (4)	0.7024 (2)
O5	0.3499 (3)	1.2016 (4)	0.7053 (2)
O6	0.1557 (3)	1.3297 (3)	0.8261 (2)
O7	0.1404 (4)	1.0259 (3)	0.8580 (2)
O8	0.2125 (4)	1.4317 (4)	0.6357 (2)
O9	−0.0747 (4)	1.4467 (3)	0.7633 (2)
O10	−0.1327 (4)	1.4106 (3)	0.5883 (2)
C	0.0297 (4)	1.1821 (4)	0.6913 (2)
C1	0.0500 (4)	1.2112 (4)	0.6348 (2)
C2	−0.1660 (5)	1.0705 (4)	0.7628 (2)
C3	−0.1017 (4)	1.2047 (4)	0.8167 (3)
C4	−0.2157 (5)	1.2498 (5)	0.7179 (3)
C5	0.2581 (5)	1.1976 (4)	0.7244 (2)
C6	0.1387 (5)	1.2775 (4)	0.7984 (3)
C7	0.1312 (5)	1.0869 (4)	0.8154 (3)
C8	0.1327 (5)	1.3899 (4)	0.6562 (3)
C9	−0.0394 (5)	1.3996 (5)	0.7337 (3)
C10	−0.0790 (5)	1.3785 (4)	0.6275 (3)

NMR (CD_2Cl_2 20 °C): 218.8 (9CO), 180.4 (Cα, $^1J_{CC}$ = 74 Hz), 68.9 (C_β, $^1J_{CC}$ = 74 Hz) ppm. Anal. Calcd (found) for $Fe_3CuIO_{10}P_4N_2C_{84}H_{62}Cl_2$: Fe, 9.25 (9.16); Cu, 3.51 (3.78); C, 55.67 (53.95); H, 3.45 (3.54).[13]

Synthesis of $[PPN]_2[Ru_3CuI(CO)_9(CCO)]$ (IV). This was prepared in manner analogous to that used for III except that the starting cluster was 150 mg (0.09 mmol) $[PPN]_2[Ru_3(CO)_9(CCO)]$: 75 mg isolated; 44% yield. IR ν(CO) (CH_3CN): 2037 (s), 1995 (s), 1975 (vs), 1926 (m), 1786 (m) cm^{-1}. ^{13}C NMR (CD_2Cl_2, −90 °C): 266.5 (3 CO), 201.9 (3 CO), 200.0 (3 CO), 157.3 (C_β, $^1J_{CC}$ = 95 Hz), −27.8 (Cα, $^1J_{CC}$ = 96 Hz) ppm. Anal. Calcd (found) for $Ru_3CuIO_{10}P_4N_2C_{83}H_{60}$: Ru, 16.28 (16.31); Cu, 3.41 (3.25); C, 53.51 (53.04); H 3.25, (3.38).

X-ray Crystal Structures of $[PPN]_2[Fe_3CuI(CO)_9(CCO)]$ (III) and $[PPN]_2[Ru_3CuI(CO)_9(CCO)]$ (IV). Crystals of both III and IV were grown by the slow diffusion of ether in CH_2Cl_2 solutions of the clusters. Fragments of suitable size were cut from larger crystals, mounted using oil (Paratone-n, Exxon) on a thin glass fiber, and cooled to −120 °C in the nitrogen stream on an Enraf-Nonius CAD4 diffractometer. Relevant collection parameters are listed in Table I. Both data sets were corrected for Lorentz, polarization, and anomalous dispersion effects. Numerical absorption corrections[14] were applied with transmission factors in the range 0.690–0.907 for III and 0.533–0.856 for IV.

The structures were solved by direct methods (SHELXS-86).[15] Correct positions for the iodine and metal atoms were deduced from an *E*-map. Subsequent least-squares–difference Fourier calculations revealed atomic positions for the remaining non-hydrogen atoms and, in the case of III, the dichloromethane solvent molecule. Hydrogen atoms were included as fixed contributors in idealized positions.

For the determination of III, in the final cycle of the least-squares fit, anisotropic thermal coefficients were refined for the non-hydrogen atoms and isotropic thermal parameters were allowed to vary for the hydrogen atoms. Successful refinement was indicated by a shift/error of 0.019, $R(F)$ = 0.038 and $R_w(F)$ = 0.042. The final positional parameters are given in Table II.

In the case of IV, one of the PPN cations was disordered on and off the 3-fold axis; consequently, the phenyl rings off the 3-fold axis were not located. In the final cycle of least-squares refinement, isotropic thermal parameters were refined for the disordered phenyl rings on the 3-fold axis. A group isotropic thermal parameter was varied for the hydrogen atoms, and the remaining non-hydrogen atoms were refined with anisotropic thermal coefficients. An isotropic extinction parameter was refined. Successful refinement was indicated by a shift/error of 0.093, $R(F)$ = 0.073, and $R_w(F)$ = 0.096. A final analysis of variance between observed and calculated structure factors showed a slight inverse dependence on sin θ. Positional parameters are given in Table III.

Table III. Positional Parameters for $[PPN]_2[Ru_3CuI(CO)_9(CCO)]$ (IV)

	x/a	y/b	z/c
I	0.3333	0.6667	0.5460 (7)
Ru	0.19813 (9)	0.5968 (1)	0.37143 (9)
Cu	0.3333	0.6667	0.4529 (1)
O1	0.0394 (10)	0.529 (1)	0.4626 (5)
O2	0.001 (1)	0.487 (2)	0.2988 (6)
O3	0.187 (1)	0.3638 (9)	0.3808 (5)
O4	0.3333	0.6667	0.2283 (9)
C1	0.104 (1)	0.550 (1)	0.4282 (6)
C2	0.076 (1)	0.531 (1)	0.3291 (6)
C3	0.236 (2)	0.464 (1)	0.3767 (6)
C4	0.3333	0.6667	0.2693 (8)
C5	0.3333	0.6667	0.317 (1)
P1	0.3333	0.6667	0.0650 (3)
P2	0.3333	0.6667	−0.0521 (3)
N1	0.3333	0.6667	0.010 (1)
C6	0.412 (1)	0.601 (2)	0.0925 (7)
C7	0.399 (2)	0.504 (2)	0.0668 (8)
C8	0.460 (2)	0.458 (2)	0.0857 (7)
C9	0.511 (2)	0.485 (2)	0.1281 (9)
C10	0.525 (2)	0.582 (2)	0.152 (1)
C11	0.471 (2)	0.637 (2)	0.1339 (8)
C12	0.267 (2)	0.525 (1)	−0.0775 (6)
C13	0.164 (2)	0.447 (2)	−0.0522 (10)
C14	0.101 (2)	0.331 (2)	−0.074 (1)
C15	0.149 (2)	0.309 (2)	−0.113 (2)
C16	0.260 (2)	0.387 (2)	−0.138 (1)
C17	0.309 (2)	0.499 (2)	−0.1200 (8)
P3	0.0	0.0	0.1859 (4)
P4	0.0	0.0	0.0715 (4)
N2	0.0	0.0	0.1287 (4)
C18	0.064 (1)	0.1420 (6)	0.2078 (6)
C19	0.169	0.2182	0.1871
C20	0.232	0.3267	0.2074
C21	0.190	0.3589	0.2484
C22	0.085	0.2826	0.2691
C23	0.022	0.1741	0.2488
C24	0.1430 (6)	0.076 (1)	0.0508 (6)
C25	0.2243	0.050	0.0673
C26	0.3313	0.102	0.0450
C27	0.3570	0.181	0.0063
C28	0.2756	0.207	−0.0102
C29	0.1686	0.155	0.0121
P5	0.118 (1)	0.065 (2)	0.150 (1)
P6	−0.1229 (7)	−0.054 (2)	0.114 (1)

Job's Law Absorption Studies. The addition of $[Cu(NCCH_3)_4][PF_6]$, PPh_3, and $P(OMe)_3$ to $[PPN]_2[Fe_3(CO)_9(CCO)]$ was studied by solution spectroscopy. Separate equimolar solutions (0.02 M) of $[PPN]_2[Fe_3(CO)_9(CCO)]$, $[Cu(NCCH_3)_4][PF_6]$, and PPh_3 in acetonitrile were employed. Mixtures were then prepared of I (1.0 mL) and varying amounts of $[Cu(NCCH_3)_4][PF_6]$ (0.50, 0.75, 1.0, 1.125, 1.25, 1.50, and 2.0 mL). If the acetonitrile ligand was to be replaced, PPh_3 or $P(OMe)_3$ was added in amounts equimolar to the copper, and the total volume was adjusted with CH_3CN. Absorption IR spectra were taken of each mixture. The intensity of the strongest ν(CO) peak of the resulting product at 1962 cm^{-1} was plotted against the ratio of the concentrations of the two starting materials: $[[Cu(NCCH_3)_4]^+]/[[Fe_3(CO)_9(CCO)]^{2-}]$.

Results

The products III and IV arising from coordination of the ketenylidene complexes I and II by ICu, eqs 1 and 2, were characterized by infrared spectroscopy and ^{13}C NMR spectroscopy. Solution ^{13}C NMR data for III and IV show that the ketenylidene ligands remain intact in solution. The solution ^{13}C NMR spectrum of III contains resonances for the cluster at 218.8 ppm (9 CO) and at 180.4 (C_β) and 68.9 ppm (C_α, $^1J_{CC}$ = 74 Hz). The resonances for the carbonyls and C_β are only shifted by a few ppm from those of I at 222.3 and 182.2 ppm,[6b] but the C_α resonance shifts from 90.1 ppm. The value of $^1J_{cc}$ observed for III is unchanged from I.

The change in chemical shift of the C_α resonance upon Cu^+ addition is the distinguishing factor between the ^{13}C NMR spectra of III and IV. The spectrum of IV is very similar to that of the

(13) The subsequent X-ray crystal structure determination shows that the crystal contains one molecule of CH_2Cl_2 per formula unit of cluster.
(14) Busing, W. R.; Levy, H. A. *Acta Crystallogr.* **1957**, *10*, 180.
(15) Sheldrick, G. M. SHELXS86: a program for crystal structure determination. University of Gottingen, Germany, 1986.

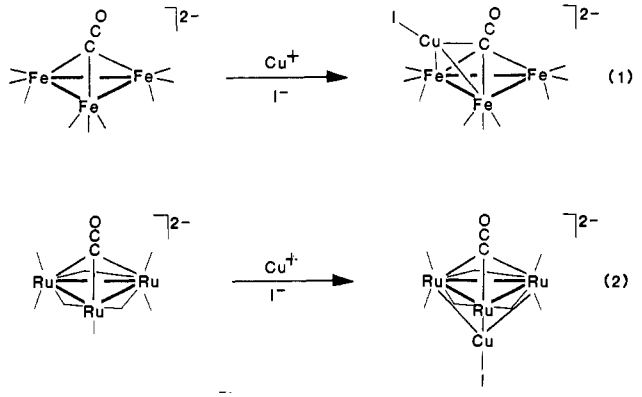

original ruthenium ketenylidene. At −90 °C, the resonances for the bridging carbonyls appear at 266.5 ppm and those for the terminal carbonyls at 201.9 and 200.0 ppm. These compare well with the carbonyl resonances of ruthenium ketenylidene (273.3, 204.0, and 202.3, respectively). The resonance for C_α of IV appears at 157.3 ppm and that for C_β appears at −27.8 ppm ($^1J_{cc}$ = 96 Hz), which compare with 159.1 and −28.3 ppm ($^1J_{cc}$ = 96 Hz) for the parent cluster.[4] In this case there is no significant shift for the C_α resonance, because its local environment is unchanged.

If residual [PPN][Cl] remains from the preparation of II, the chloride displaces acetonitrile from the added Cu^+ before other ligands can be added. The resulting chloride adduct was isolated as a crystalline solid as described for IV, and was characterized by NMR spectroscopy. The resonances for the cluster carbons in $[PPN]_2[Ru_3CuCl(CO)_9(CCO)]$ are at 268.0, 200.9, 199.8, 157.5, and −29.5 ppm ($^1J_{cc}$ = 96 Hz), nearly identical to those of IV.

Infrared spectra reveal the expected increase in ν(CO) associated with the addition of a Lewis acid when Cu^+ adds to the cluster ketenylidenes, Table IV. The isolated and structurally characterized adducts III and IV, which contain CuI, are clearly present in solution (Table IV). In addition, the shifts in ν(CO) indicate the formation of Cu^+L^+ adducts of I where L = acetonitrile, triphenylphosphine, or trimethyl phosphite. The resulting cluster adducts with neutral ligands could not be precipitated from solution as crystalline solids. However, the intensity of a strong band at 1962 cm^{-1} common to all three species grows, with increasing LCu^+ loading, at the expense of bands due to I, up to a LCu^+:$[Fe_3(CO)_9(CCO)]^-$ ratio of 1:1. The Job's law plots of the data for $[Fe_3CuL(CO)_9(CCO)]^-$ [L = CH_3CN (solvent), Hg–PPh_3, $P(OMe)_3$] are shown in Figure 1.

These data confirm that formation of a stable $[Fe_3CuL(CO)_9(CCO)]^-$ adduct from Cu^+ and I proceeds with a variety of ligands. The subsequent addition of iodide therefore simply effects a ligand exchange on cluster-bound Cu^+ to afford the dianion III, which is more readily crystallized than the acetonitrile, phosphine, or phosphite complexes because of differing solubility. The same is presumed to be true of $[Ru_3CuL(CO)_9CCO]^{-/2-}$ adducts, but only IV was investigated. All the Cu^+ adducts, including III and IV are freely soluble in CH_3CN and CH_2Cl_2.

A drop in the intensity of the 1962-cm^{-1} bands beyond a 1:1 LCu^+ addition, Figure 1, suggests possible addition of a second Cu^+ to the clusters at higher loadings. In CH_2Cl_2 solution, IR spectroscopy reveals bands at still higher frequency for both the iron and ruthenium ketenylidenes when excess Cu^+ is added. The spectra display similar ν(C≡O) bands near 1997 cm^{-1}, and the products can be completely extracted from PPN^+ with low-polarity solvents. These observations suggest the formation of $M_3Cu_2L_2(CO)_9(CCO)$ species. However, in the more coordinating solvent CH_3CN, a different ν(CO) pattern is observed, indicating that the presumed bis(copper) complexes have limited stability.

In summary, these results indicate that at a 1:1 LCu^+:$[M_3(CO)_9(CCO)]^{2-}$ ratio, the predominant species is $[M_3CuL(CO)_9(CCO)]^{-/2-}$ for a wide variety of ligands, and there is evidence for the formation of clusters containing a higher proportion of copper.

Table IV. IR Frequencies ν(CO) (cm^{-1})[a]

$[M_3(CO)_9(CCO)]^{2-}$	$[M_3Cu(NCCH_3)(CO)_9(CCO)]^-$	$[M_3Cu(PPh_3)(CO)_9(CCO)]^{2-}$	$[M_3CuI(CO)_9(CCO)]^{2-}$
	M = Fe		
	2049 (2)	2049 (w)[b]	2024 (m)
		2033 (m)	
1924 (s)	1963 (s)	1963 (s)	1952 (s)
1872 (m)	1883 (w)	1878 (m)	1877 (m)
	M = Ru		
2023 (m)	2060 (m)[b]	2041 (m)[b]	2037 (s)[b]
1982 (s)	2011 (s)	1994 (s)	1995 (s)
1952 (vs)	1999 (vs)	1976 (vs)	1975 (vs)
1899 (m)	1940 (m)	1928 (m)	1926 (m)
1750 (m, br)	1788 (w, br)	1788 (m, br)	1786 (m, br)

[a] CH_2Cl_2 solutions, except as noted. [b] CH_3CN solutions.

Table V. Bond Lengths (Å) and Selected Bond Angles (deg) for $[PPN]_2[Fe_3CuI(CO)_9(CCO)]$ (III)

	Bond Lengths		
Fe1–Fe2	2.605 (1)	C6–O6	1.141 (7)
Fe2–Fe3	2.575 (1)	C7–O7	1.162 (7)
Fe1–Fe3	2.554 (1)	C8–O8	1.156 (8)
Cu–Fe1	2.552 (1)	C9–O9	1.148 (8)
Cu–Fe2	2.551 (1)	C10–O10	1.142 (8)
Cu–C	2.008 (5)	Fe1–C2	1.763 (6)
Fe1–C	1.955 (5)	Fe1–C3	1.761 (6)
Fe2–C	1.971 (5)	Fe1–C4	1.755 (6)
Fe3–C	2.046 (5)	Fe2–C5	1.769 (6)
C–C1	1.317 (8)	Fe2–C6	1.777 (6)
C1–O1	1.180 (7)	Fe3–C8	1.748 (6)
C2–O2	1.162 (7)	Fe3–C9	1.786 (6)
C3–O3	1.167 (7)	Fe3–C10	1.782 (6)
C4–O4	1.164 (8)	Cu–I	2.4377 (8)
C5–O5	1.159 (7)	Fe2–C7	1.776 (6)
	Bond Angles		
Fe1–Fe2–Fe3	59.07 (3)	Cu–C–Fe3	152.4 (3)
Fe1–Fe3–Fe2	61.05 (3)	Fe1–C–Fe2	83.1 (2)
Fe2–Fe1–Fe3	59.88 (3)	Fe1–C–Fe3	79.3 (2)
Fe1–Cu–Fe2	61.39 (3)	Fe2–C–Fe3	79.7 (2)
Cu–Fe1–Fe2	59.28 (3)	C–C1–O1	167.0 (6)
Cu–Fe2–Fe1	59.33 (3)	Fe1–C2–O2	169.5 (5)
Fe1–Cu–I	149.67 (4)	Fe1–C3–O3	177.3 (5)
Fe2–Cu–I	145.06 (4)	Fe1–C4–O4	175.2 (5)
Fe1–C–C1	138.4 (4)	Fe2–C5–O5	177.2 (5)
Fe2–C–C1	130.9 (4)	Fe2–C6–O6	176.3 (5)
Fe3–C–C1	84.0 (4)	Fe2–C7–O7	171.6 (5)
Cu–C–C1	123.5 (4)	Fe3–C8–O8	178.9 (6)
I–Cu–C	151.0 (2)	Fe3–C9–O9	177.8 (6)
Cu–C–Fe1	80.2 (2)	Fe3–C10–O10	176.8 (6)
Cu–C–Fe2	79.8 (2)		

Mass spectrometry studies were done on the heterometallic systems. For III, a peak at *m/e* 650 for the parent dianion is followed by the successive loss of three carbonyls. Redistribution of Cu^+ gives iron ketenylidene at *m/e* 460 with further loss of two carbonyls, and a peak at *m/e* 712 is assigned to a cluster containing two Cu^+ associated with $[Fe_3(CO)_9CCO]^{2-}$. For $[Ru_3CuI(CO)_9(CCO)]^{2-}$ the parent peak at *m/e* 786 is followed by the successive loss of three carbonyls. Again there is loss of CuI to give ruthenium ketenylidene at *m/e* 598, accompanied by the loss of five carbonyls. A minor unidentified peak was observed at *m/e* 1040.

An X-ray structure determination revealed that the addition of Cu^+ to I results in formation of a four-metal butterfly cluster with a μ_4-CCO ligand, Figure 2. The heterometal is found at a wingtip position. The average M-M bond distance of the iron triangle 2.578(1) Å in III is unchanged compared to the starting material, as are the C-C1 and C1-O1 distances of the CCO ligand (1.317(8) and 1.180(7) Å, respectively), Table V. The ketenylidene ligand is decidedly bent, ∠CCO = 167.0 (6)°, compared to the original iron ketenylidene, ∠CCO = 172.8 (23)°.[10] The Cu–C_α separation of 2.008 (5) Å is well within bonding distance.

While the copper can be thought of as capping a triangular Fe_2C face in III, it caps a Ru_3 face in IV Figure 3. The cluster is now

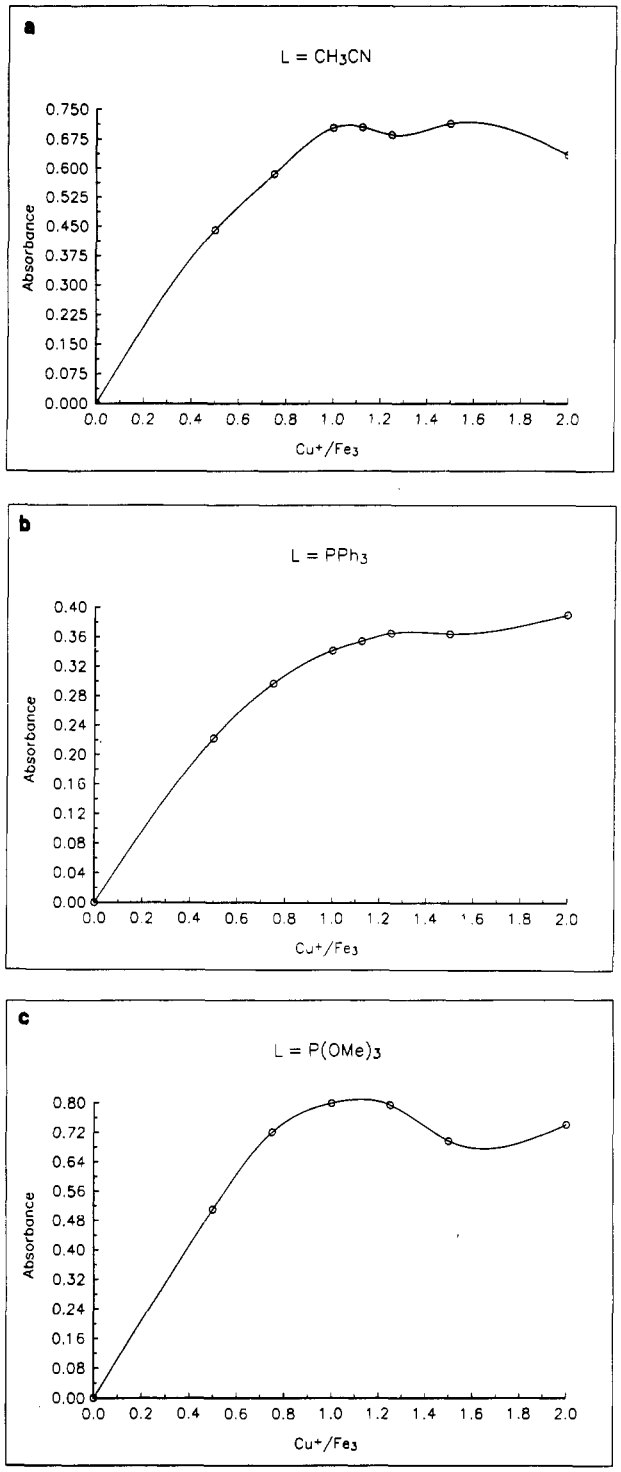

Figure 1. Job's law plots of absorbance of $[Fe_3CuL(CO)_9CCO)]^{2-}$ vs the concentration ratio $[LCu^+]:[Fe_3(CO)_9(CCO)]^{2-}$ for L = CH_3CN (a), PPh_3 (b), and $P(OMe)_3$ (c).

highly symmetrical with a 3-fold axis running through the CCO and CuI moieties on opposite sides of the Ru_3 triangle. The ruthenium metal atoms are separated by 2.770 (2) Å, Table VI. The distance from each ruthenium to the face-capping copper is 2.677 (3) Å. As in II, six terminal and three bridging carbonyls are present. The Ru–CO distances are 1.84 (2), 1.86 (2), and 2.12 (1) Å, respectively. Although the Ru–Ru and Ru–CO bond distances are similar to those of the parent ketenylidene, there are slight differences in the dimensions of the ketenylidene ligand itself.

Discussion

The difference in the modes of attack by Cu^+ on I and II may be the result of the differences in the structures of the starting materials or differences in the metal basicity of Fe and Ru. The metal framework of iron ketenylidene is fairly inaccessible because three of the nine terminal carbonyls are axial. For the ruthenium ketenylidene the bridging carbonyls give access to the metal

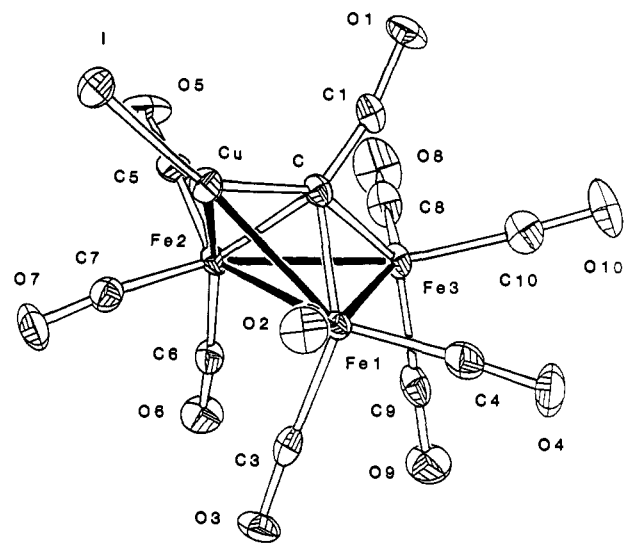

Figure 2. ORTEP drawing of the cluster dianion in $[PPN]_2[Fe_3CuI(CO)_9(CCO)]$ (III), with ellipsoids drawn at 35% probability.

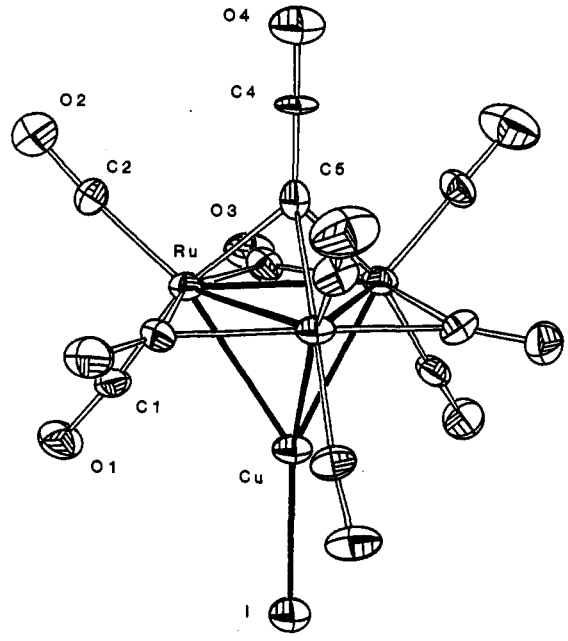

Figure 3. ORTEP drawing of the cluster dianion in $[PPN]_2[Ru_3CuI(CO)_9(CCO)]$ (IV), with 35% probability ellipsoids.

Table VI. Bond Lengths (Å) and Selected Bond Angles (deg) for $[PPN]_2[Ru_3CuI(CO)_9(CCO)]$ (IV)

	Bond Distances		
Ru–Ru	2.770 (2)	Cu–I	2.454 (3)
Ru–Cu	2.677 (3)	C5–C4	1.25 (4)
Ru–C1	1.86 (2)	C1–O1	1.20 (2)
Ru–C2	1.82 (2)	C2–O2	1.20 (2)
Ru–C3	2.12 (1)	C3–O3	1.19 (2)
Ru–C5	2.15 (2)	C4–O4	1.08 (3)
	Bond Angles		
Ru–Cu–I	143.34 (6)	Cu–Ru–C3	80.4 (4)
Ru–C1–O1	172 (1)	Cu–Ru–C5	95.4 (6)
Ru–C2–O2	175 (1)	Cu–Ru–Ru′	58.8 (5)
Ru–C3–O3	139 (1)	C1–Ru–C2	91.2 (7)
Ru–C5–C4	132.0 (6)	C1–Ru–C3	94.3 (7)
Ru–C5–Ru′	81.5 (6)	C1–Ru–C5	168.5 (8)
Ru–C3–Ru′	81.6 (6)	C2–Ru–C3	100.0 (6)
Cu–Ru–C1	73.2 (5)	C2–Ru–C5	100.2 (8)
Cu–Ru–C2	164.4 (5)	C3–Ru–C5	84.4 (5)

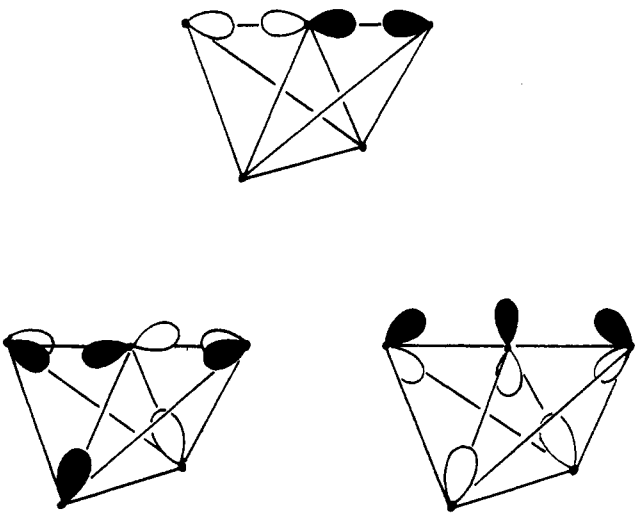

Figure 4. Diagram of a butterfly carbide framework, illustrating the interaction of carbon p orbitals with metal framework orbitals.[18a]

triangle opposite the ketenylidene ligand.[3] In addition, the attack of copper on C_α of iron ketenylidene is facilitated by the 33° tilt of the ligand from perpendicular. In the case of ruthenium ketenylidene, this tilt is only 12° and the ligand is therefore less accessible.[5]

The structures of III and IV can be understood in terms of polyhedral skeletal electron pair theory.[16] Addition of LCu^+, with no electron pairs, to the *nido*-M_3C_α tetrahedra of I and II is expected to produce *closo*-CuM_3C_α trigonal bipyramids. Copper can add to the M_3 face as in IV, or to one of the M_2C faces as in III. In both instances, Cu^+ occupies an axial position on the resulting closed framework, but C_α can be in cis-equatorial or trans-axial positions; both possible structural isomers are represented by III and IV, respectively. However, description of the structures on this basis requires a Cu–C_α bond in III.

Further evidence of a Cu–C_α interaction in III beyond that already discussed above is provided by the disposition of the iodide ligand on the copper. If the sp-hybridized Cu^+ were simply bridging the hinge irons, the I^- ligand should reside in the plane of the three metals. Instead, the Cu–I bond lies 12.0° below this plane toward the carbonyl ligands, despite the large ionic radius of I^-. This suggests that the copper sp acceptor orbitals are directed away from the hinge toward C_α. A greater involvement of the Cu^+ p orbitals could also be invoked to explain the displacement of I^-, but the geometry about copper is decidedly removed from tetrahedral or even trigonal planar.

An interesting comparison can be made between the addition of copper versus other electrophiles. The isolobal analogy[17] between $CuL^{+/0}$ and H^+ is often invoked because of similar reactivity.[7] In the presence case, Cu^+ addition to iron ketenylidene does not cleave the CCO ligand as seen for H^+. However, the reaction patterns are similar with the ruthenium ketenylidene, where Cu^+ caps the Ru_3 triangle and H^+ spans a Ru–Ru edge. Compound III may represent an intermediate or transition state in the protonation of the iron ketenylidene. Thus H^+ may attack an Fe_2C face, followed by the displacement of the ketenylidene CO to form a methylidyne. The driving force for the latter step would be the relatively high strength of the C–H bond in the product.

Butterfly carbides such as $[Fe_4C(CO)_{12}]^{2-}$ are thought to have strong M(wingtip)–C–M(wingtip) π and σ interactions, Figure 4.[18] Copper(I) with its low-energy filled d orbitals cannot participate in the strong M–C $d\pi$–$p\pi$ interaction required to stabilize a carbide, and this accounts for the retention of the CCO ligand in the ketenylidene $[Fe_3CuI(CO)_9(CCO)]^{2-}$.

Acknowledgment. Support for this research came from the NSF-Synthetic Inorganic Organometallic Program and the Pew Great Lakes Cluster Science program.

Supplementary Material Available: Tables giving a summary of the X-ray data collection, thermal parameters, and hydrogen atom positional parameters for IV (2 pages); a complete list of structure factors for IV (15 pages). Ordering information is given on any current masthead page.

(16) (a) Wade, K. *Adv. Inorg. Chem. Radiochem.* **1975**, *18*, 1. (b) Mingos, D. M. P. *Adv. Organomet. Chem.* **1977**, *15*, 1. (c) Lauher, J. W. *J. Am. Chem. Soc.* **1978**, *100*, 5305.

(17) Hoffmann, R. *Science*, **1981**, *21*, 995.

(18) (a) Harris, S.; Bradley, J. S. *Organometallics* **1984**, *3*, 1086. (b) Hriljac, J. A.; Harris, S.; Shriver, D. F. *Inorg. Chem.* **1988**, *27*, 816.